A Paclitaxel-Hyaluronan Bioconjugate Targeting Ovarian Cancer Affords a Potent *In vivo* Therapeutic Activity

Alessandra Banzato,[1] Sara Bobisse,[1] Maria Rondina,[1] Davide Renier,[5] Fabio Bettella,[5] Giovanni Esposito,[4] Luigi Quintieri,[2] Laura Meléndez-Alafort,[3] Ulderico Mazzi,[3] Paola Zanovello,[1,4] and Antonio Rosato[1,4]

Abstract

Purpose: This study was designed to evaluate the pharmacologic and biological properties of a paclitaxel-hyaluronan bioconjugate (ONCOFID-P) against IGROV-1 and OVCAR-3 human ovarian cancer xenografts following i.p. administration.

Experimental Design: *In vitro* tumor sensitivity to ONCOFID-P was analyzed by the 3-(4,5-dimethylthiazol-2-yl)-2,5-diphenyltetrazolium bromide assay, whereas bioconjugate interaction with cells was studied cytofluorimetrically and by confocal microscopy. *In vivo* toxicity was assessed by a single-dose maximum-tolerated dose, peripheral blood cell count determination and by histologic analysis. Biodistribution of the compound was evaluated with a small animal–dedicated scintigraphy gamma camera following injection of ^{99m}Tc-labeled ONCOFID-P. Pharmacokinetic analysis was also carried out. Female severe combined immunodeficiency mice implanted with ovarian cancer cells underwent treatment with ONCOFID-P or free paclitaxel starting from day 7 or 14 after tumor injection, and survivals were compared.

Results: ONCOFID-P interacted with CD44, entered cells through a receptor-mediated mechanism, and exerted a concentration-dependent inhibitory effect against tumor cell growth. After i.p. administration, the bioconjugate distributed quite uniformly within the peritoneal cavity, was well-tolerated, and was not associated with local histologic toxicity. Pharmacokinetic studies revealed that blood levels of bioconjugate-derived paclitaxel were much higher and persisted longer than those obtained with the unconjugated free drug. Intraperitoneal treatment of tumor-bearing mice with the bioconjugate revealed that ONCOFID-P exerted a relevant increase in therapeutic activity compared with free drug.

Conclusions: ONCOFID-P significantly improved results obtained with conventional paclitaxel, in terms of *in vivo* tolerability and therapeutic efficacy; these data strongly support its development for locoregional treatment of ovarian cancer.

Ovarian cancer is the most common cause of death from gynecologic malignancy and is the fifth leading cause of cancer-related death (1). Intravenous administration of taxane- and platinum-based chemotherapy represents the current standard of postoperative care for patients with advanced neoplasia. This therapeutic regimen is also considered for high-risk patients with early stage tumors in an adjuvant setting, to eradicate residual disease following surgical debulking. Despite these approaches having resulted in improved survival over the last decade, nonetheless, relapses still occur in the majority of cases and represent the major problem for patients with advanced disease (2).

A potential solution to these obstacles takes into consideration the biological behavior of ovarian cancer, which is mainly confined to the peritoneal cavity for most of its initial natural course. The biology of the tumor offers the possibility of delivering drugs directly within the peritoneum to achieve a theoretical potential for increased exposure of the tumor to the antineoplastic agents, leading to improved cytotoxic effects and a higher therapeutic effect. Moreover, this local route of administration may blunt some of the more severe systemic effects of high-dose i.v. treatment, and the depot effect could also serve as a reservoir for systemic resorption resulting in longer systemic drug exposure (3–6). In this regard, an ideal candidate antitumor drug for intraperitoneal therapy should present several characteristics such as a documented efficacy against the neoplasia to be treated, clinical or experimental evidence for concentration-dependent cytotoxicity, good tolerability and low toxicity for the peritoneal lining following regional delivery, slow exit from the peritoneal cavity and rapid clearance from the systemic circulation, and relevant and rapid

Authors' Affiliations: Departments of [1]Oncology and Surgical Sciences, [2]Pharmacology and Anesthesiology, and [3]Pharmaceutical Sciences, University of Padova, [4]Istituto Oncologico Veneto, Padua, Italy, and [5]Fidia Farmaceutici, Abano Terme, Italy

Received 8/15/07; revised 12/3/07; accepted 12/27/07.

Grant support: Azione Biotech 2005-Regione Veneto, and Fidia Farmaceutici (A. Rosato). A. Banzato is a fellow of the Italian Association for Cancer Research.

The costs of publication of this article were defrayed in part by the payment of page charges. This article must therefore be hereby marked *advertisement* in accordance with 18 U.S.C. Section 1734 solely to indicate this fact.

The funding sources had no role in the study design, data collection, data analysis, data interpretation, or writing of this report.

Requests for reprints: Antonio Rosato, Department of Oncology and Surgical Sciences, University of Padova, Via Gattamelata 64, I-35128 Padua, Italy. Phone: 39-49821-5800, ext. 8215858; Fax: 39-49807-2854; E-mail: antonio.rosato@unipd.it.

doi:10.1158/1078-0432.CCR-07-2019

liver metabolism to a nontoxic metabolite thus increasing the pharmacokinetic advantage associated with regional delivery and decreasing the risks of systemic side effects (7).

Macromolecular drug delivery systems have been proposed as a potential tool to overcome drug resistance, to improve the therapeutic index, and to increase tolerability. Polymeric conjugates of chemotherapy agents are internalized by endocytosis and accumulate in lysosomes thus allowing the drug to be released from polymers closer to molecular targets and rendering it less susceptible to membrane-linked drug efflux mechanisms. Moreover, whereas free drugs readily extravasate to normal tissues, the size of drug copolymers restrict such distribution, potentially decreasing toxicity. On the other hand, these macromolecules still retain the capacity to cross the leaky, irregular vasculature of solid neoplasia and to accumulate in the tumor interstitium (8–11).

Hyaluronan, a linear polysaccharide formed by alternating D-glucuronic acid (GlcUA) and *N*-acetyl-D-glucosamine (GlcNAc) units, is present in the extracellular matrix, the synovial fluid of joints, and the scaffolding that comprises cartilage. Hyaluronan interacts with proteins playing crucial roles in cell adhesion, growth, and migration, and acts as a signaling molecule in cell motility, inflammation, wound healing, and cancer metastasis (12). Several types of cellular receptors respond to hyaluronan as a signal. These include CD44, a family of glycoproteins originally associated with lymphocyte activation (13), RHAMM, the receptors for hyaluronan-mediated cell motility (14), and HARE, which is responsible for receptor-mediated uptake of hyaluronan in liver (15). Because hyaluronan receptors (CD44, RHAMM) are overexpressed in a wide variety of cancers including ovarian tumors (16–22), hyaluronan-drug bioconjugates should present a markedly enhanced selectivity for cancerous cells, providing, at the same time, advantages in drug solubilization, stabilization, localization, and controlled release. Hyaluronan has already been conjugated to different antineoplastic drugs, generating new compounds with promising antitumor effects (23–26).

In the present report, we show that biological and pharmacologic properties of ONCOFID-P, a new hyaluronan-paclitaxel bioconjugate (27), are well-suited to locoregional application in the treatment of ovarian cancer, leading to enhanced therapeutic effectiveness.

Materials and Methods

Drugs. The preparation of the hyaluronan-paclitaxel bioconjugate (Fidia Farmaceutici) with ~20% of paclitaxel loading has been previously described (27). Formerly indicated as HYTAD1-p20, it is hereafter reported as ONCOFID-P. Paclitaxel (taxol) was from Bristol-Myers Squibb Italia.

Mice and tumor cell lines. Six- to 8-week-old female severe combined immunodeficiency (SCID) and BALB/c mice were purchased from Charles River Laboratories (Calco), and housed in our specific-pathogen–free animal facility. Procedures involving animals and their care were in conformity with institutional guidelines that comply with national and international laws and policies. IGROV-1 and OVCAR-3 human ovarian cancer cell lines were cultured in RPMI 1640 (EuroClone) supplemented with 2 mmol/L of L-glutamine (Life Technologies), 10 mmol/L of HEPES (PAA Laboratories), 150 units/mL of streptomycin (Bristol-Mayers Squibb Italia), 200 units/mL of penicillin (Pharmacia & Upjohn), 1 mmol/L of sodium pyruvate, and 10% (v/v) heat-inactivated FCS (Life Technologies).

3-(4,5-Dimethylthiazol-2-yl)-2,5-diphenyltetrazolium bromide assay. The *in vitro* cytotoxicity of ONCOFID-P and paclitaxel was studied in IGROV-1 and OVCAR-3 cells using a previously described 3-(4,5-dimethylthiazol-2-yl)-2,5-diphenyltetrazolium bromide assay (28). Within each experiment, determinations were done in triplicate, and experiments were repeated 10 times. IC_{50} values were calculated from semilogarithmic dose-response curves by linear interpolation and reported as mean ± SD. In competition experiments, cells were preincubated with a dose escalation excess of high-molecular weight hyaluronan (analogous to that used for ONCOFID-P synthesis) for 2 h before the addition of a single dose (1 μg/mL) of bioconjugate.

Cell staining and flow cytometry analysis. CD44 expression on IGROV-1 and OVCAR-3 cells was investigated by flow cytometry, as previously reported (27). Evaluation of CD44 modulation upon interaction with ONCOFID-P or hyaluronan was carried out by incubating ovarian cancer cells (3×10^5/sample) in 1 mL of complete medium containing 500 μg/mL of ONCOFID-P or hyaluronan at 37°C. At different time points, cells were harvested as previously described (27) and receptor expression was compared with that of unstimulated cells.

Labeling of ONCOFID-P with BODIPY and confocal microscopy analysis. For the labeling of the bioconjugate with the fluorochrome, 400 μL of a 5 mg/mL water solution of BODIPY [5-([(4-[4,4-difluoro-5-(2-thienyl)-4-bora-3a,4a-diaza-s-indacene-3-yl]phenoxy)acetyl]amino) pentylamine, hydrochloride, BODIPY TR cadaverine; Molecular Probes] were added to a solution of ONCOFID-P (40 mg in 15 mL of water). After the addition of 1.6 μL of triethylamine, 1.68 mg of *N*-hydroxyl succinimide and 2.82 mg of 1-ethyl-3-(3-dimethylaminopropyl)carbodiimide hydrochloride were added and pH was maintained at 7.4, in order to allow amide bond formation between BODIPY and the carboxylic groups of the hyaluronan derivative. The reaction mixture was left to stand at room temperature for 24 h and then extensively dialyzed. The pure product was freeze-dried, resuspended in water at 10 mg/mL, and then tested in a 3-(4,5-dimethylthiazol-2-yl)-2,5-diphenyltetrazolium bromide assay to verify its cytotoxicity against ovarian cancer cells. The labeled product and free ONCOFID-P showed similar IC_{50} values (data not shown). To assess the interaction of the labeled bioconjugate with ovarian cancer cells, IGROV-1 and OVCAR-3 cells were seeded on glass coverslips in 12-well tissue culture plates at a concentration of 8×10^5 cells/well. After 24 h, the cells were supplemented with 50 μg/mL of BODIPY-ONCOFID-P for 2 h, fixed for 20 min in 4% formaldehyde, and then analyzed. For lysosomal colocalization studies, ovarian cancer cells were cultivated using the Lab-Tek chambered no. 1.0 borosilicate coverglass system (Nalge Nunc International). After 24 h of culture, cells were incubated with Lyso Tracker Green DND-26 (50 nmol/L; Molecular Probes) for 30 min at 37°C, and then 10 μg/mL of BODIPY-ONCOFID-P was added during the analysis. To visualize microtubules, ovarian cancer cells were prepared on coverslips and incubated with paclitaxel (100 μg/mL) or ONCOFID-P (100 μg/mL paclitaxel equivalents) for 4 h. After fixation and permeabilization for 20 min with 0.1% NP40/PBS, the cells were incubated with an anti-human β-tubulin mouse monoclonal antibody (Sigma-Aldrich) for 45 min, followed by staining with anti-mouse immunoglobulin Alexa 546-conjugated goat antiserum (Molecular Probes). Sample analysis was carried out with a Zeiss LSM 510 microscope (Carl Zeiss) using argon (488 nm) and helium-neon (543 nm) lasers with objectives and settings as specified in the figure legends. Laser intensity, pinhole aperture, and photomultiplier variables were standardized to allow the comparison of signals obtained in different samples. Fluorescence signals were analyzed using a 505- to 530-nm bandpass filter for Lyso Tracker Green and a longpass 560 nm filter for BODIPY and immunoglobulin Alexa 546 signals. Quantitation was carried out with Zeiss's profile software tool. Field-merging was visualized by red and green false-color overlay.

Evaluation of maximum-tolerated dose of ONCOFID-P. Survey experiments to define the single-dose maximum-tolerated dose (MTD) in BALB/c and SCID mice were conducted with five animals

per group. Groups of mice received i.p. 20, 40, 80, 90, 100, 110, or 120 mg/kg paclitaxel equivalent of ONCOFID-P. Mice survival and variation in body weight were observed daily over 30 days in all groups. The MTD was defined as the allowance of a median body weight loss of 15% of the weight before pharmacologic treatments and causes neither death due to toxic effects nor remarkable changes in the general signs within 1 week after administration. Animals showing weight loss exceeding 20% were sacrificed.

Assessment of bone marrow toxicity. Groups of healthy BALB/c mice (n = 12/group) were treated on day 0 with a single-dose MTD of ONCOFID-P i.p. or paclitaxel i.v. On days 4, 7, 11, and 20, heparinized retro-orbital sinus blood samples were collected and leukocytes counted with a hemocytometer after lysis of RBC with PUREGENE RBC Lysis Solution (Gentra Systems). Results were analyzed using the Mann-Whitney test.

Local tolerability analysis. To assess the potential irritating effects of ONCOFID-P and free paclitaxel on the peritoneal mesothelium, BALB/c mice (n = 10/group) were treated once i.p. with either drug at the MTD. At different time points thereafter (at 3, 7, and 24 h, and at 5 and 7 days), two animals per time point were sacrificed and fragments of their abdominal wall were collected for morphologic analysis. For histologic evaluation, tissue samples were fixed in 4% neutral-buffered formalin, embedded in paraffin, sectioned at 4 μm, and stained with H&E staining.

Labeling of ONCOFID-P with ^{99m}Tc and biodistribution studies with the yttrium-aluminum-perovskite camera. ONCOFID-P was labeled with ^{99m}Tc according to a previously described protocol (29). *In vivo* biodistribution of ^{99m}Tc-ONCOFID-P was evaluated in female BALB/c mice using a small animal–dedicated yttrium-aluminum-perovskite (YAP) camera (29, 30). Briefly, mice were anesthetized by a mix of ketamine and xylazine (100 and 10 mg/kg, respectively). Three hundred microliters of ^{99m}Tc-ONCOFID-P (~6-8 MBq) were then injected i.p. Scintigraphic images were collected by the YAP camera for 2 h (10-min accumulation for each image). At the end of image collection, animals were sacrificed and the total gamma-ray activity of each organ was measured to determine the *ex vivo* biodistribution of the radiolabeled complex. Values were expressed as the percentage of injected activity (%IA).

Pharmacokinetics studies and high-performance liquid chromatography analysis of plasma paclitaxel content. To determine plasma pharmacokinetics following i.p. administration, mice were injected with ONCOFID-P (n = 19; 40 mg/kg of paclitaxel equivalent) or paclitaxel (n = 39; 40 mg/kg). Heparinized venous blood samples (80 μL/sample/mouse) were collected and pooled before drug administration and at different time points thereafter during a 6-day period. Plasma was separated by centrifugation and immediately frozen at -20°C after collection. For drug quantification, 200 μL of plasma was placed in a thermostatic bath at 30°C for 1 h after the addition of 0.1 mol/L of NaOH (200 μL). Paclitaxel and its metabolites were extracted with 7 mL of diethyl ether, the mixture fully evaporated, diluted in 200 μL of acetonitrile/water (1:1) and analyzed by high-performance liquid chromatography.

Tumor challenge. SCID mice were inoculated i.p. with 5×10^6 IGROV-1 or OVCAR-3 tumor cells. Pharmacologic treatments were started at day 7 or day 14 from tumor injection and carried out according to a q7dx3 (every 7 days for three doses) or q7dx4 (every 7 days for four doses) schedule, respectively, employing a MTD of ONCOFID-P administered i.p. or of free paclitaxel injected i.v. The *in vivo* tumor growth experiments were conducted according to the U.K. Coordinating Committee on Cancer Research guidelines for the welfare of animals in experimental neoplasia (31). During *in vivo* experiments, animals in all experimental groups were examined daily for a decrease in physical activity and other signs of disease or drug toxicity; severely ill animals were euthanized by carbon dioxide overdose.

Statistical analysis. Survival curves and probabilities were estimated using the Kaplan-Meier technique. A log-rank test for comparisons was used when required. Analyses of data were done using the MedCalc statistical package (version 8.1).

Results

In vitro *tumor growth inhibition activity of ONCOFID-P against ovarian cancer cells.* To test ONCOFID-P *in vitro* efficacy against IGROV-1 and OVCAR-3 ovarian cancer lines, cells were incubated with escalating concentrations of ONCOFID-P and the dose-dependent growth inhibition was compared with that of the commercial free drug. Results showed that the antiproliferative activity of ONCOFID-P (IC_{50}, 0.64 ± 0.39 and 0.06 ± 0.11 μg/mL for IGROV-1 and OVCAR-3, respectively) was comparable or even superior to that of the unconjugated paclitaxel (IC_{50}, 0.29 ± 0.31 and 0.30 ± 0.65 μg/mL for IGROV-1 and OVCAR-3, respectively). No toxic effects could be ascribed to hyaluronan (data not shown).

Analysis of interaction of ONCOFID-P with ovarian tumor cells. Hyaluronan receptors expressed on target cells may directly interact with the bioconjugate, resulting in the uptake of ONCOFID-P by tumor cells. Flow cytometry analysis showed that CD44 receptor was intensely expressed on both IGROV-1

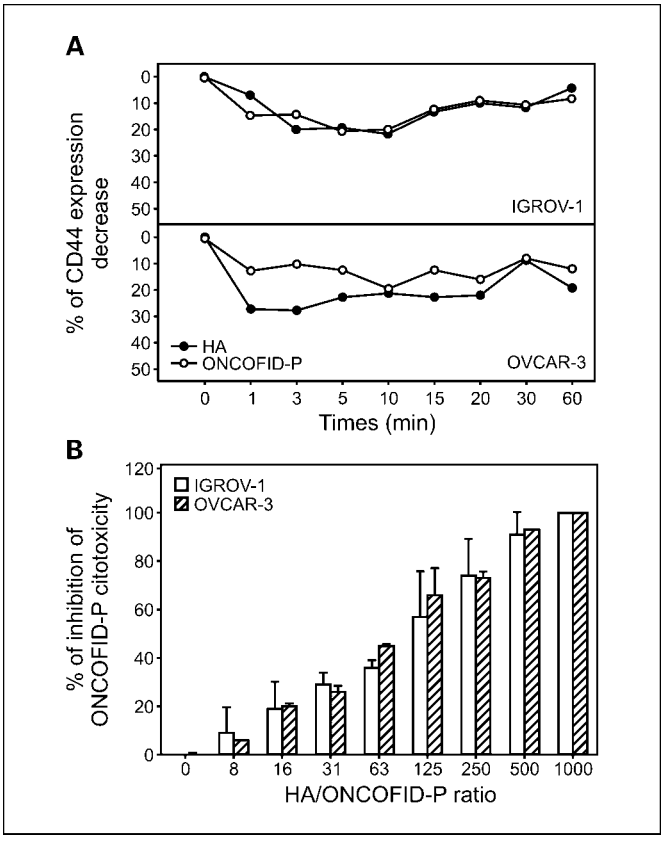

Fig. 1. ONCOFID-P interaction with ovarian cancer cells. *A,* modulation of CD44 expression upon interaction with ONCOFID-P (○) or hyaluronan (●) was evaluated by incubating ovarian cancer cells at 37°C in the presence of compounds. At different time points thereafter, cells were stained with an FITC-labeled anti-human CD44 mouse monoclonal antibody, analyzed by flow cytometry, and CD44 expression was reported as a geometric mean. *B,* functional competition of hyaluronan in reducing the cytotoxic activity of ONCOFID-P. IGROV-1 and OVCAR-3 tumor cells were preincubated with escalating doses of hyaluronan for 2 h and then a fixed dose (1 μg/mL paclitaxel equivalent) of bioconjugate was added. Tumor growth was assessed 3 d later in a 3-(4,5-dimethylthiazol-2-yl)-2,5-diphenyltetrazolium bromide assay. Columns, percentages of inhibition of bioconjugate activity at different hyaluronan/ONCOFID-P ratios on IGROV-1 (*empty columns*) and OVCAR-3 (*hatched columns*) cancer cells.

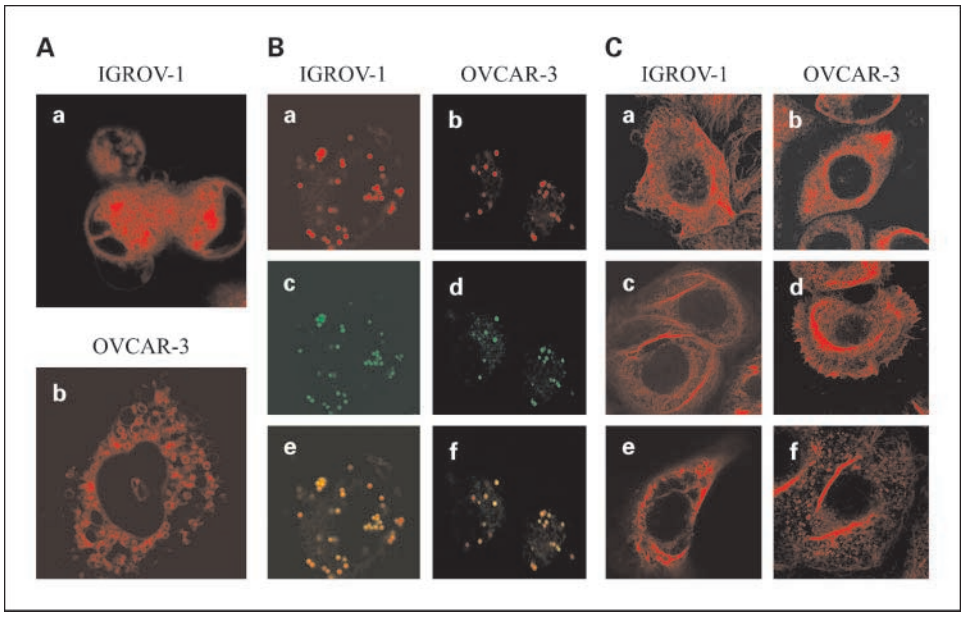

Fig. 2. Confocal microscopy analysis. *A,* ONCOFID-P accumulation in IGROV-1 (*a*) and OVCAR-3 (*b*) ovarian tumor cells. Cells were incubated with BODIPY-ONCOFID-P (50 μg/mL) for 2 h, washed and fixed before analysis. Images were captured using a 63× oil immersion objective lens (1.4 numerical aperture). *B,* colocalization analysis of ONCOFID-P in lysosomes. IGROV-1 (*a, c, e*) and OVCAR-3 (*b, d, f*) cells were labeled with LysoTracker Green and then incubated with BODIPY-ONCOFID-P (10 μg/mL). *a* and *b,* fluorescence of the labeled bioconjugate in a single cell; *c* and *d,* signals from lysosomes. The merging of the two components is visible in *e* and *f*. Lysosomes (~90% to 100%) were occupied by BODIPY-ONCOFID-P, as assessed by the Zeiss' profile software tool. *C,* rearrangement of IGROV-1 (*a, c, e*) and OVCAR-3 (*b, d, f*) cell microtubular architecture after drug treatment. Ovarian tumor cells were left untreated (*a* and *b*), or incubated for 4 h with paclitaxel (100 μg/mL; *c* and *d*) or ONCOFID-P (100 μg/mL paclitaxel equivalents; *e* and *f*). After fixation and permeabilization, cells were stained with an anti-human β-tubulin mouse monoclonal antibody followed by anti-mouse immunoglobulin Alexa 546–conjugated secondary antibody. Images were taken as reported in (*A*) with an electronic zoom factor of 2.9.

and OVCAR-3 cancer cell lines (data not shown). Because chemical coupling of paclitaxel to hyaluronan might affect the binding of ONCOFID-P to CD44, IGROV-1 and OVCAR-3 cells were incubated with either the bioconjugate or hyaluronan, and CD44 expression was then analyzed at different time points. Exposure of both cell lines to either hyaluronan or ONCOFID-P induced a rapid and transient down-modulation in CD44 expression, thus demonstrating a specific interaction of the hyaluronan moiety with the receptor (Fig. 1A). To assess whether hyaluronan-binding receptors/ONCOFID-P direct interaction is involved in the intracellular specific uptake of the bioconjugate, we analyzed the survival of ovarian cancer cell lines following exposure to ONCOFID-P or free paclitaxel in the absence or in the presence of escalating doses of hyaluronan. Results established that increasing concentrations of hyaluronan competed and displaced ONCOFID-P from binding receptors leading to a dose-dependent reduction of bioconjugate cytotoxicity thus indicating that direct interaction of the compound with binding receptors plays an important role in the cytotoxic activity of ONCOFID-P (Fig. 1B). Conversely, the efficacy of free drug was unaffected by hyaluronan (data not shown).

Labeling of ONCOFID-P with BODIPY, a red-emitting fluorochrome, allowed us to directly visualize the intracellular accumulation of the bioconjugate (Fig. 2A), which produced a dotted pattern verisimilarly due to sequestration into lysosomes (12, 32). Indeed, confocal microscopy analysis of IGROV-1 and OVCAR-3 tumor cells loaded with a green fluorescent lysosome tracker and treated with BODIPY-labeled ONCOFID-P clearly showed that the bioconjugate did accumulate in the lysosomal compartment (Fig. 2B). Thereafter, the enzymatic content of these organelles is likely responsible for the degradation of the hyaluronan moiety and also for the breakdown of the carboxyl ester link between hyaluronan and paclitaxel, which in turn, is released in a full active form in the cytoplasm and is capable of interfering with the microtubule polymerization dynamics, as shown by the formation of bundles similar to those induced by treatment with free drug (Fig. 2C).

Intraperitoneal ONCOFID-P exhibits a lower host toxicity than free paclitaxel and presents an elevated local tolerability. To assess the potentiality of the i.p. administration route, we first evaluated the MTD of ONCOFID-P. Groups of BALB/c and SCID mice were inoculated i.p. with different amounts of drug (20, 40, 80, 90, 100, 110, and 120 mg/kg of paclitaxel equivalent) and monitored for weight loss over the following days. Results showed that the 100 mg/kg paclitaxel equivalent dose of ONCOFID-P brought about an average acute weight loss of 9.8%; lower concentrations of drug had negligible effects whereas higher dosages were associated with weight loss of >15%, producing results that were too toxic (Fig. 3A). Therefore, the 100 mg/kg paclitaxel equivalent dose was assumed as the single-dose MTD for ONCOFID-P through the i.p. route. Moreover, in our hands, the single-dose MTD for free paclitaxel was, respectively, 20 and 10 mg/kg for the i.v. and the i.p. administration routes (data not shown); therefore, results showed that the bioconjugate allowed for a 5- to 10-fold increase in paclitaxel dose deliverable for therapeutic purposes.

Myelosuppression is a major dose-limiting toxicity of many anticancer agents, including paclitaxel. To determine the bone marrow toxicity of ONCOFID-P, peripheral WBC counts were taken in healthy BALB/c mice at day 0, before drug inoculation,

and on days 4, 7, 10, 15, and 30 after administration of single-dose MTD of ONCOFID-P i.p. or free paclitaxel i.v. Mice receiving free paclitaxel showed a marked myelosuppression that lasted for at least 2 weeks (59%, 23%, 67%, and 64% decrease in WBC counts on days 4, 7, 10, and 15, respectively) and recovered in ~1 month (Fig. 3B). WBC counts were not significantly different in mice treated with ONCOFID-P versus free paclitaxel at all tested points, except at day 30 ($P = 0.0097$) when leukocytes had not fully recovered yet. No differences in WBC counts were observed in mice receiving hyaluronan alone, whereas cremophor brought about a dramatic WBC increase, likely due to its irritating and inflammatory properties (data not shown).

To assess whether ONCOFID-P induced irritating effects in the peritoneal mesothelial lining, two groups of BALB/c mice received a single-dose MTD i.p. injection of the bioconjugate or cremophor-formulated paclitaxel. Small portions of the abdominal wall were then removed at different time points after drug administration for histologic examination. Histopathology showed no inflammatory infiltrate in ONCOFID-P–treated mesothelium. Furthermore, direct contact of the compound with the mucosa apparently did not induce other morphologic changes in the mesothelial lining at any time point analyzed (Fig. 4A and C; data not shown). Conversely, mice treated with free paclitaxel displayed an inflammatory reaction and a leukocyte infiltration at both the mesothelial lining and the underlying muscle abdominal wall. Such features were already present at 7 h after drug inoculation, peaked at 24 h, and then progressively disappeared (Fig. 4B and D; data not shown). These results indicate that ONCOFID-P is extremely well-tolerated by the mesothelium and was not associated with significant inflammatory effects.

Biodistribution studies and pharmacokinetic analysis of ONCOFID-P following i.p. administration. We then studied the biodistribution of the bioconjugate following i.p. administration using a small animal–dedicated scintigraphy YAP camera. The biodistribution was assessed on anesthetized mice placed in the field of view of the YAP camera for 2 h after ^{99m}Tc-ONCOFID-P administration (Fig. 5A). Images obtained at time intervals of 10 min revealed that essentially only the peritoneal cavity provided a detectable scintigraphic signal. Radioactivity distribution seemed quite uniform thus indicating that the injected material did not remain confined to the inoculation site. Intraperitoneal organs could not be specifically visualized and this suggested that they did not accumulate labeled material (Fig. 5B-D). This feature was further shown at the end of the experiment, when animals were sacrificed and the radioactivity accumulated in their organs was directly measured. Extraperitoneal organs presented negligible values of radioactivity whereas intraperitoneal organs, such as the stomach, intestine, kidneys, liver, and spleen were associated with higher signals (3-7% of the injected activity each), verisimilarly due to the mucoadhesive properties of ONCOFID-P that adhered to the external mesothelium. However, almost 70% of the radioactive signal was retained in the carcass, likely in association with the parietal mesothelial lining (Fig. 5E).

Nevertheless, this distribution data may have actually identified the presence of the hyaluronan moiety, which was directly labeled with ^{99m}Tc, and not the conjugated paclitaxel. Indeed, it was possible that dissociation took place *in vivo* in the peritoneal cavity, leading to the production of free paclitaxel or paclitaxel-coupled small hyaluronan oligomers that could traverse the mesothelial barrier and enter the bloodstream. To assess this possibility, a pharmacokinetic analysis was carried out following ONCOFID-P i.p. administration to mice. Groups of 10 animals treated i.p. with either ONCOFID-P (40 mg/kg paclitaxel equivalent) or free paclitaxel (40 mg/kg) as a control, underwent serial blood sampling before and after drug administration in order to determine plasma concentrations of paclitaxel by high-performance liquid chromatography analysis. Plasma concentrations of paclitaxel following free drug administration peaked in 6 hours and were almost negligible at 24 h (area under the curve value = 144 μg h/mL). Conversely, ONCOFID-P administration brought about a striking increase in paclitaxel plasma levels (area under the curve value = 1,069 μg h/mL). Indeed, values in paclitaxel plasma concentration increased with a slightly slower kinetics in comparison to free drug, reached a plateau in ~24 h, that lasted up to 48 h, and declined slowly in the following days returning to basal levels only at 120 h (Fig. 5F).

Antitumor* in vivo *efficacy. In the first set of experiments, SCID mice were injected i.p. with IGROV-1 ovarian cancer cells,

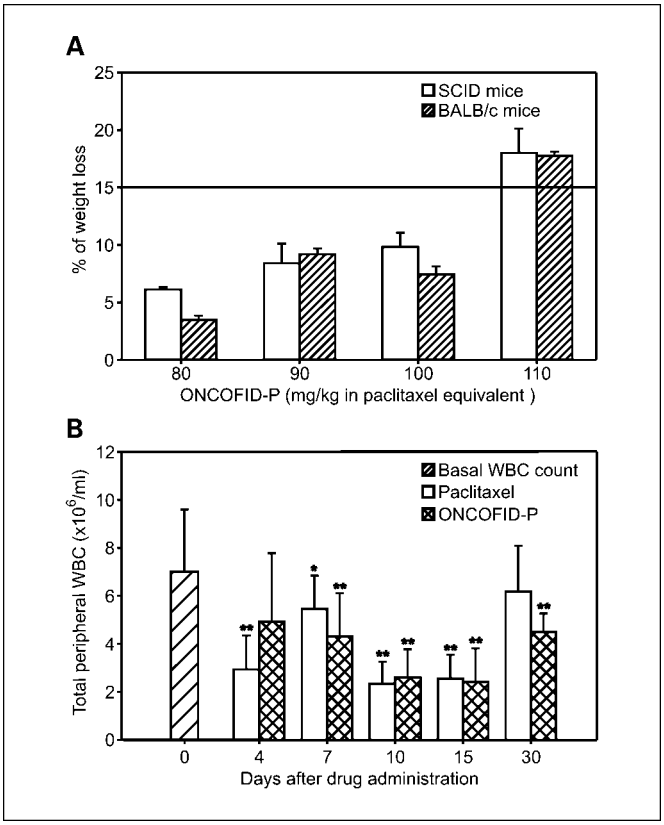

Fig. 3. *A,* assessment of ONCOFID-P single-dose MTD after i.p. administration. Columns, mean from a group of five SCID (*empty columns*) or BALB/c (*hatched columns*) mice receiving a single-dose of 80, 90, 100, or 110 mg/kg of paclitaxel equivalents of ONCOFID-P; bars, SE. The MTD was defined as the allowance of a median body weight loss of 15% of the weight before pharmacologic treatments. *B,* myelosuppression studies in healthy BALB/c animals inoculated with ONCOFID-P or free paclitaxel. Mice ($n = 12$/group) were treated with the single-dose MTD of either ONCOFID-P (100 mg/kg paclitaxel equivalent i.p.) or free paclitaxel (20 mg/kg i.v.) once. Columns, mean of total peripheral WBC counts evaluated at day 0 (*hatched columns*), before treatment, and 4, 7, 10, 15, and 30 d later (*empty columns*, paclitaxel; *cross-hatched columns*, ONCOFID-P); bars, SE (*, $P < 0.05$ vs. basal levels; **, $P < 0.01$ vs. basal levels).

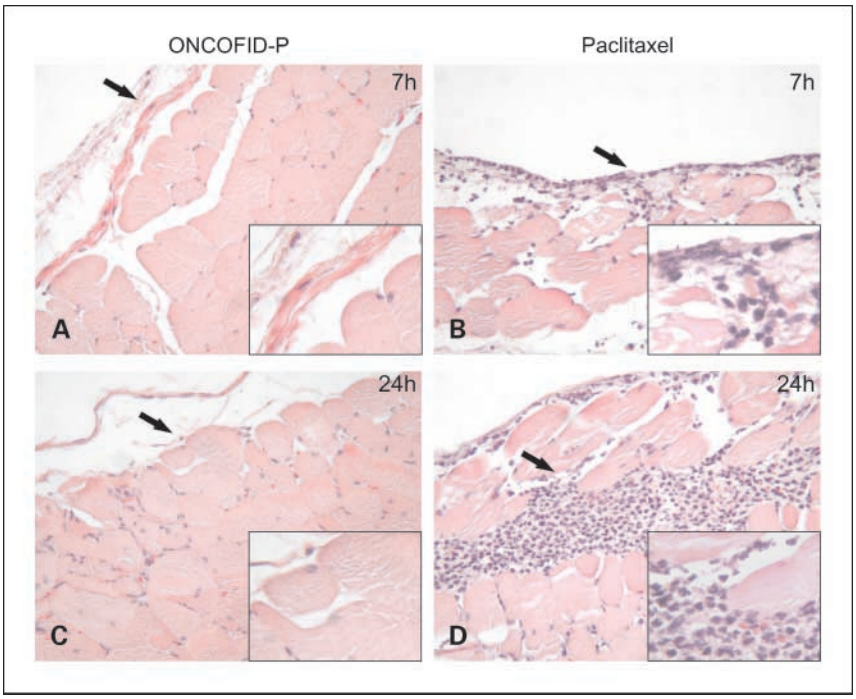

Fig. 4. Local tolerability study. Histologic analyses were carried out on abdominal wall samples at different time points after i.p. administration of a single-dose MTD of ONCOFID-P (*A* and *C*) or cremophor-formulated paclitaxel (*B* and *D*). Effects after 7 h (*A* and *B*) and 24 h (*C* and *D*). H&E staining (original magnification, ×20). Insets, a more detailed view of the area indicated by the arrow (magnification, ×40).

a very aggressive tumor with a rapid growth rate, and treated i.p. with escalating doses of ONCOFID-P (10, 20, 40, and 80 mg/kg paclitaxel equivalent). Results showed a dose-dependent therapeutic activity with increasing survival in comparison with untreated control mice (data not shown).

I.p. administration of paclitaxel for ovarian cancer therapy is gaining increasing interest and results of recent clinical trials have produced remarkable data (3–6); however, the requirement of cremophor as a solvent has important drawbacks, due to its irritating and toxic properties (33, 34), that limit the i.p. administrable dose in comparison to the i.v. route. Therefore, we decided to compare the therapeutic efficacy of multiple MTDs of ONCOFID-P (100 mg/kg paclitaxel equivalent) given i.p. with that induced by MTDs of paclitaxel (20 mg/kg) injected i.v., which still represents the standard route of administration of the drug. To this end, SCID mice (n = 12/group) were inoculated i.p. with IGROV-1 or OVCAR-3 cancer cells at day 0, treated with MTDs of ONCOFID-P or paclitaxel at days 7, 14, and 21 (q7dx3 schedule), and survival to tumor challenge was monitored. In IGROV-1–bearing mice, ONCOFID-P–treated animals (median survival, 52 days) underwent a strong therapeutic benefit and presented a 2.9-fold and 2.5-fold increase in survival in comparison to untreated control mice (median survival, 18 days; $P < 0.0001$) and free paclitaxel-treated animals (median survival, 21 days; $P < 0.0001$), respectively (Fig. 6A). Free paclitaxel brought about a slight improvement in survival that however was not significant ($P = 0.0785$ versus control; Fig. 6A). Similar results were also obtained using OVCAR-3, a tumor with a slower rate of *in vivo* growth (Fig. 6C). In this case, free paclitaxel-treated mice had a significant therapeutic effect (median survival, 83 days), resulting in a 1.6-fold increase in survival in comparison to untreated control mice (median survival, 52 days; $P < 0.0001$). On the other hand, ONCOFID-P was extremely efficient in contrasting tumor growth in mice treated with the bioconjugate (median survival, 164 days), and determined a 3.2-fold and 2-fold increase in survival in comparison to control ($P < 0.0001$) and paclitaxel-treated mice ($P < 0.0001$), respectively. In this experimental context, we also compared the therapeutic effects induced by i.p. treatment with MTDs of free paclitaxel; in particular, in mice bearing IGROV-1 tumors, this approach (median survival, 43 days) increased effectiveness in comparison to free drug given i.v. ($P < 0.0001$), but was still less efficient than ONCOFID-P administration ($P < 0.0001$).

An increased therapeutic effectiveness was also observed when pharmacologic treatment was started 14 days after tumor inoculation and adopting a more aggressive regimen (q7dx4 schedule). Indeed, in mice bearing IGROV-1 tumors, bioconjugate treatment resulted in a median survival of 53 days, which was significantly higher than that observed in free paclitaxel–treated (median survival, 30 days, 1.8-fold increase; $P = 0.0041$) and control (median survival, 27 days, 2-fold increase; $P = 0.0015$) mice (Fig. 6B). Paclitaxel alone did not increase survival in comparison to untreated animals ($P = 0.2232$). Finally, Fig. 6D shows that OVCAR-3–bearing ONCOFID-P–treated mice (median survival, 141 days) presented a significantly longer survival than animals receiving free paclitaxel (median survival, 95 days, 1.5-fold increase; $P = 0.0001$) or control mice (median survival, 53 days, 2.7-fold increase; $P = 0.0042$). Although the median survival of paclitaxel-treated and control mice were different, the results were not significant ($P = 0.1955$). No therapeutic activity was induced by treatment with either cremophor or hyaluronan alone (data not shown).

Discussion

I.p. administration of antineoplastic drugs has already been investigated in phase I, II, and III clinical trials for safety, pharmacology, and efficacy, and have shown a therapeutic benefit in patients with ovarian cancer (3–6). In this regard,

paclitaxel has shown an important pharmacokinetic advantage after i.p. regional delivery; however, severe concerns still exist about local toxicity that limits the use of appropriate drug amounts, thus leading to a reduced concentration of systemic exposure in comparison with i.v. therapy. Toxic aspects are likely due to cremophor, a component of taxol's commercial formulation, which is essential for solubilization but is also responsible for several side effects and adverse drug reactions (33, 34).

To overcome the limitations of paclitaxel related to the solvent and to increase its therapeutic effects, the agent was incorporated into microspheres, nanospheres, and liposomes (35–37), formulations providing a continued, slow drug release. Moreover, significant advancements have been made by encapsulation of paclitaxel into bioadhesive microspheres (38) that promote sustained release of the drug or by formulating paclitaxel in copolymers using D,L-lactide, polyethylene glycol, and poly-L-glutamic acid, with the aim of reducing toxicity and increasing localization to tumor implants and antitumor efficacy in comparison to free paclitaxel (39–43).

We previously reported that conjugation of paclitaxel with hyaluronan led to the generation of a new chemical entity endowed with efficient antineoplastic activity and high tissue tolerability, and that was characterized by a potential new mechanism of interaction with target cells. This latter aspect has been particularly investigated in the present report. Indeed, ONCOFID-P penetration and efficacy within cells appeared due to the active interaction of the hyaluronan moiety with surface hyaluronan receptors, as assessed by (*a*) the CD44 modulation upon interaction with bioconjugate, (*b*) the dose-dependent inhibition of ONCOFID-P activity in the presence of increasing amounts of hyaluronan, (*c*) the direct visualization of bioconjugate accumulation into cells and its compartmentalization in lysosomes, and (*d*) the analysis of effects induced on the microtubule apparatus. Such data are in line with and extend the results of previous reports demonstrating that similar paclitaxel-hyaluronan conjugates underwent uptake by hyaluronan receptor–expressing tumor cells; thus, inducing selective cytotoxicity upon hydrolytic release of the active paclitaxel in intracellular compartments (23, 24, 26). These aspects are particularly relevant when we consider the wide expression of CD44 and other hyaluronan receptors in ovarian cancers (16–22).

A critical requirement for drugs to be used for intraabdominal chemotherapy is tissue tolerability and negligible toxicity for the mesothelial lining. Accordingly, no apparent signs of inflammation or morphologic changes were detected at the histologic analysis following ONCOFID-P i.p. administration. These favorable aspects are likely due to the relatively high water-solubility of the conjugate, which eliminates the need for

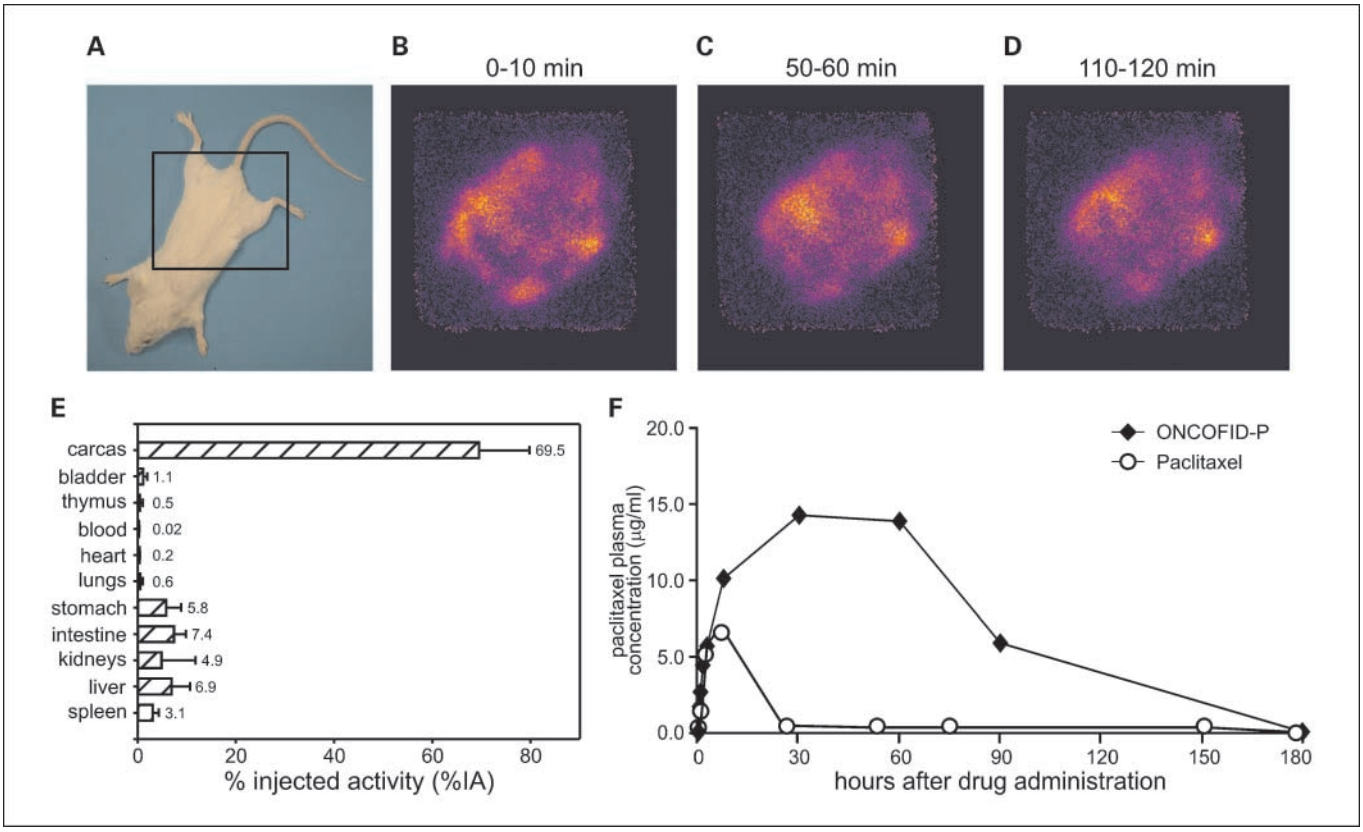

Fig. 5. Biodistribution and pharmacokinetic studies of ONCOFID-P. *A, in vivo* distribution of ^{99m}Tc-labeled ONCOFID-P was investigated using a high-spatial resolution YAP gamma camera (a mouse undergoing imaging and the field of view of the gamma camera). *B* to *D,* scintigraphic images collected at different time points after i.p. inoculation of the radioactive compound (one representative mouse is illustrated). *E,* at the completion of experiments, animals were sacrificed and radioactivity accumulated in organs was directly measured. Columns, mean obtained in three experiments; bars, SE. *F,* plasma pharmacokinetics following drug administration was assessed in mice injected i.p. with ONCOFID-P (n = 19, 40 mg/kg paclitaxel equivalent) or paclitaxel (n = 39, 40 mg/kg). Heparinized venous blood samples were collected and pooled before drug administration and at different time points thereafter during a 6-day period. Plasma paclitaxel content was determined by high-performance liquid chromatography. Area under the curve values: paclitaxel, 144 μg h/mL; ONCOFID-P, 1,069 μg h/mL.

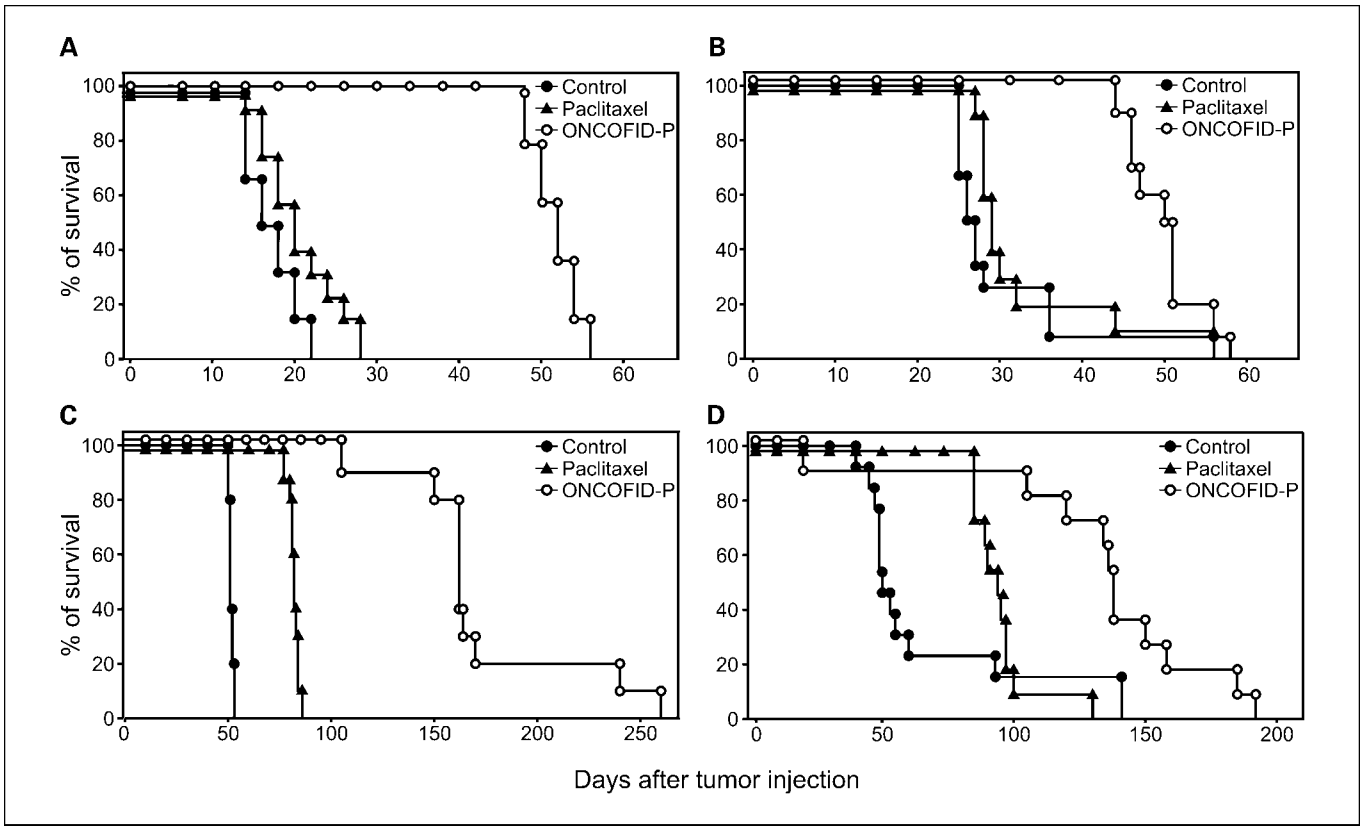

Fig. 6. *In vivo* therapeutic activity of ONCOFID-P against human ovarian tumor growth. Kaplan-Meier survival curves of mice inoculated with IGROV-1 (*A* and *B*) or OVCAR-3 (*C* and *D*) cancer cells. Tumors were induced by i.p. injection of 5×10^6 ovarian cancer cells in SCID mice (day 0). Seven (*A* and *C*) or 14 (*B* and *D*) days later, animals were randomly assigned to an experimental group and drug treatment was initiated according to therapeutic schedules reported in Materials and Methods. Mice were left untreated (controls, $n = 12$; ●) or received paclitaxel (20 mg/kg i.v., $n = 12$, ▲) or ONCOFID-P (100 mg/kg paclitaxel equivalent i.p., $n = 12$, ○). Statistical analysis: *A,* ONCOFID-P vs. controls, $P < 0.0001$; paclitaxel vs. controls, $P = 0.0785$; ONCOFID-P vs. paclitaxel, $P < 0.0001$. *B,* ONCOFID-P vs. controls, $P = 0.0015$; paclitaxel vs. controls, $P = 0.2232$; ONCOFID-P vs. paclitaxel, $P = 0.0041$. *C,* ONCOFID-P vs. controls, $P < 0.0001$; paclitaxel vs. controls, $P < 0.0001$; ONCOFID-P vs. paclitaxel, $P < 0.0001$. *D,* ONCOFID-P vs. controls, $P = 0.0042$; paclitaxel vs. controls, $P = 0.1955$; ONCOFID-P vs. paclitaxel, $P = 0.0001$.

cremophor as a solvent and its irritating properties, and due to the high profile of biocompatibility of the hyaluronan moiety which is extensively used in a cross-linked format to prevent postoperative adhesions following major abdominal surgical interventions (44). Moreover, the hyaluronan backbone likely provides additional advantages for i.p. regional therapeutic application against tumor nodules implanted at the mesothelial lining during tumor diffusion, as strong mucoadhesion has been reported for a ≈200 kDa grade hyaluronan, a product very similar to that used for ONCOFID-P synthesis (45). On the other hand, the excellent tissue tolerability allowed for a 5-fold to 10-fold increase in the amount of administrable paclitaxel, which in turn, could translate into a deeper therapeutic effect.

A fundamental goal of intraperitoneal chemotherapy is to increase exposure of the locally growing neoplasia to elevated drug concentrations while minimizing systemic toxic effects. The results of *in vivo* imaging with a radiolabeled compound showed an intraperitoneal sequestration of bioconjugate at least during the first few hours after inoculation. More importantly, pharmacokinetic data showed a slow degradation/release of ONCOFID-P in the circulation, bringing about sustained and persistent levels of free paclitaxel in the blood. At this point, the high-performance liquid chromatography extraction method by which paclitaxel is quantified in blood does not allow a precise discrimination between free drug and paclitaxel still coupled to hyaluronan oligomers produced by ONCOFID-P i.p. degradation and capable of passing the peritoneal lining and entering the bloodstream. However, if we consider the levels of bone marrow toxicity and the lack of neuropathy, it is hard to sustain that the elevated levels of paclitaxel present in the blood are ascribable only to free drug. A more likely hypothesis considers a slow degradation of ONCOFID-P followed by release of oligomers in the bloodstream where they undergo rapid hepatic uptake. Therefore, it is very likely that the i.p. injected bioconjugate remains available for interaction with tumor cells for several days; this aspect, in conjunction with the wide expression of CD44 and RHAMM receptors on ovarian cancer cells, constituting a binding site for ONCOFID-P that thereby could preferentially target neoplastic tissue and spare the surrounding normal tissue, is likely responsible of the high therapeutic effect produced by ONCOFID-P. Accordingly, overall survival was strongly increased in two different compartmental models of human ovarian carcinoma using ONCOFID-P i.p. as compared with free paclitaxel i.v., both being administered at equitoxic levels, a study approach that was chosen because the i.v. route for paclitaxel still represents the standard. Nonetheless, the bioconjugate showed a superior therapeutic profile even when both ONCOFID-P and free paclitaxel were given i.p at MTDs. Interestingly, the therapeutic activity of ONCOFID-P against

OVCAR-3 tumor cells seemed more favorable to that exerted by a poly-L-glutamic acid–paclitaxel copolymer (43) or another paclitaxel-hyaluronan conjugate (26) when used against the OVCAR-3–derived cisplatin-resistant NMP-1 ovarian tumor cell line, even though, in the latter case, differences in the schedule and doses of administration preclude a direct comparison.

In conclusion, the scenario we favor is that intraperitoneal ONCOFID-P behaves as a depot system which is highly tolerated by the mesothelial lining and leads to very high drug concentrations just close to tumor cells, which, in turn, incorporate the bioconjugate through an active mechanism, thus ultimately resulting in an increased therapeutic effectiveness. Therefore, we believe that ONCOFID-P represents a significant improvement over conventional paclitaxel and can be considered as a potential important new tool that is particularly well-suited for intraperitoneal chemotherapy against ovarian cancer.

Acknowledgments

We thank V. Barbieri for excellent technical assistance; G. Moschini and G. Giron for providing access to the YAP camera facility; and M. Bello for expert assistance with scintigraphic image collection.

References

1. Barnes MN, Grizzle WE, Grubbs CJ, Partridge EE. Paradigms for primary prevention of ovarian carcinoma. CA Cancer J Clin 2002;52:216–25.
2. Cannistra SA. Cancer of the ovary. N Engl J Med 2004;351:2519–29.
3. Muggia FM. New and emerging intraperitoneal (IP) drugs for ovarian cancer treatment. Semin Oncol 2006;33:S18–24.
4. Fujiwara K, Armstrong D, Morgan M, Markman M. Principles and practice of intraperitoneal chemotherapy for ovarian cancer. Int J Gynecol Cancer 2007;17:1–20.
5. Petignat P, du Bois A, Bruchim I, Fink D, Provencher DM. Should intraperitoneal chemotherapy be considered as standard first-line treatment in advanced stage ovarian cancer? Crit Rev Oncol Hematol 2007;62:137–47.
6. Rao G, Crispens M, Rothenberg ML. Intraperitoneal chemotherapy for ovarian cancer: overview and perspective. J Clin Oncol 2007;25:2867–72.
7. Markman M. Intraperitoneal antineoplastic drug delivery: rationale and results. Lancet Oncol 2003;4:277–83.
8. Greish K, Fang J, Inutsuka T, Nagamitsu A, Maeda H. Macromolecular therapeutics: advantages and prospects with special emphasis on solid tumour targeting. Clin Pharmacokinet 2003;42:1089–105.
9. Mehvar R. Recent trends in the use of polysaccharides for improved delivery of therapeutic agents: pharmacokinetic and pharmacodynamic perspectives. Curr Pharm Biotechnol 2003;4:283–302.
10. Jaracz S, Chen J, Kuznetsova LV, Ojima I. Recent advances in tumor-targeting anticancer drug conjugates. Bioorg Med Chem 2005;13:5043–54.
11. Duncan R. Polymer conjugates as anticancer nanomedicines. Nat Rev Cancer 2006;6:688–701.
12. Liao YH, Jones SA, Forbes B, Martin GP, Brown MB. Hyaluronan: pharmaceutical characterization and drug delivery. Drug Deliv 2005;12:327–42.
13. Marhaba R, Zoller M. CD44 in cancer progression: adhesion, migration and growth regulation. J Mol Histol 2004;35:211–31.
14. Nedvetzki S, Gonen E, Assayag N, et al. RHAMM, a receptor for hyaluronan-mediated motility, compensates for CD44 in inflamed CD44-knockout mice: a different interpretation of redundancy. Proc Natl Acad Sci U S A 2004;101:18081–6.
15. Weigel JA, Raymond RC, McGary C, Singh A, Weigel PH. A blocking antibody to the hyaluronan receptor for endocytosis (HARE) inhibits hyaluronan clearance by perfused liver. J Biol Chem 2003;278:9808–12.
16. Cannistra SA, Abu-Jawdeh G, Niloff J, et al. CD44 variant expression is a common feature of epithelial ovarian cancer: lack of association with standard prognostic factors. J Clin Oncol 1995;13:1912–21.
17. Gardner MJ, Catterall JB, Jones LM, Turner GA. Human ovarian tumour cells can bind hyaluronic acid via membrane CD44: a possible step in peritoneal metastasis. Clin Exp Metastasis 1996;14:325–34.
18. Stickeler E, Runnebaum IB, Mobus VJ, Kieback DG, Kreienberg R. Expression of CD44 standard and variant isoforms v5, v6 and v7 in human ovarian cancer cell lines. Anticancer Res 1997;17:1871–6.
19. Kayastha S, Freedman AN, Piver MS, Mukkamalla J, Romero-Guittierez M, Werness BA. Expression of the hyaluronan receptor, CD44S, in epithelial ovarian cancer is an independent predictor of survival. Clin Cancer Res 1999;5:1073–6.
20. Makrydimas G, Zagorianakou N, Zagorianakou P, Agnantis NJ. CD44 family and gynaecological cancer. In Vivo 2003;17:633–40.
21. Sillanpaa S, Anttila MA, Voutilainen K, et al. CD44 expression indicates favorable prognosis in epithelial ovarian cancer. Clin Cancer Res 2003;9:5318–24.
22. Zagorianakou N, Stefanou D, Makrydimas G, et al. CD44s expression, in benign, borderline and malignant tumors of ovarian surface epithelium. Correlation with p53, steroid receptor status, proliferative indices (PCNA, MIB1) and survival. Anticancer Res 2004;24:1665–70.
23. Luo Y, Prestwich GD. Synthesis and selective cytotoxicity of a hyaluronic acid-antitumor bioconjugate. Bioconjug Chem 1999;10:755–63.
24. Luo Y, Ziebell MR, Prestwich GD. A hyaluronic acid-taxol antitumor bioconjugate targeted to cancer cells. Biomacromolecules 2000;1:208–18.
25. Luo Y, Bernshaw NJ, Lu ZR, Kopecek J, Prestwich GD. Targeted delivery of doxorubicin by HPMA copolymer-hyaluronan bioconjugates. Pharm Res 2002;19:396–402.
26. Auzenne E, Ghosh SC, Khodadadian M, et al. Hyaluronic acid-paclitaxel: antitumor efficacy against CD44(+) human ovarian carcinoma xenografts. Neoplasia 2007;9:479–86.
27. Rosato A, Banzato A, De Luca G, et al. HYTAD1-20: a new paclitaxel-hyaluronic acid hydrosoluble bioconjugate for treatment of superficial bladder cancer. Urol Oncol 2006;24:207–15.
28. Quintieri L, Rosato A, Napoli E, et al. *In vivo* antitumor activity and host toxicity of methoxymorpholinyl doxorubicin: role of cytochrome P450 3A. Cancer Res 2000;60:3232–8.
29. Coradini D, Zorzet S, Rossin R, et al. Inhibition of hepatocellular carcinomas *in vitro* and hepatic metastases *in vivo* in mice by the histone deacetylase inhibitor HA-But. Clin Cancer Res 2004;10:4822–30.
30. Uzunov N, Bello M, Boccaccio P, et al. Performance measurements of a high-spatial-resolution YAP camera. Phys Med Biol 2005;50:N11–21.
31. UKCCCR guidelines for the welfare of animals in experimental neoplasia. Cancer Metastasis Rev 1989;8:82–8.
32. Stern R. Hyaluronan catabolism: a new metabolic pathway. Eur J Cell Biol 2004;83:317–25.
33. Cormio G, Di Vagno G, Melilli GA, et al. Hypersensitivity reactions in ovarian cancer patients receiving paclitaxel. J Chemother 1999;11:407–9.
34. Weiss RB, Donehower RC, Wiernik PH, et al. Hypersensitivity reactions from taxol. J Clin Oncol 1990;8:1263–8.
35. Suh H, Jeong B, Rathi R, Kim SW. Regulation of smooth muscle cell proliferation using paclitaxel-loaded poly(ethylene oxide)-poly(lactide/glycolide) nanospheres. J Biomed Mater Res 1998;42:331–8.
36. Wang YM, Sato H, Adachi I, Horikoshi I. Preparation and characterization of poly(lactic-co-glycolic acid) microspheres for targeted delivery of a novel anticancer agent, taxol. Chem Pharm Bull (Tokyo) 1996;44:1935–40.
37. Harper E, Dang W, Lapidus RG, Garver RI, Jr. Enhanced efficacy of a novel controlled release paclitaxel formulation (PACLIMER delivery system) for local-regional therapy of lung cancer tumor nodules in mice. Clin Cancer Res 1999;5:4242–8.
38. Le Visage C, Rioux-Leclercq N, Haller M, Breton P, Malavaud B, Leong K. Efficacy of paclitaxel released from bio-adhesive polymer microspheres on model superficial bladder cancer. J Urol 2004;171:1324–9.
39. Zhang X, Burt HM, Mangold G, et al. Anti-tumor efficacy and biodistribution of intravenous polymeric micellar paclitaxel. Anticancer Drugs 1997;8:696–701.
40. Li C, Yu DF, Newman RA, et al. Complete regression of well-established tumors using a novel water-soluble poly(L-glutamic acid)-paclitaxel conjugate. Cancer Res 1998;58:2404–9.
41. Li C, Price JE, Milas L, et al. Antitumor activity of poly(L-glutamic acid)-paclitaxel on syngeneic and xenografted tumors. Clin Cancer Res 1999;5:891–7.
42. Jackson JK, Gleave ME, Yago V, Beraldi E, Hunter WL, Burt HM. The suppression of human prostate tumor growth in mice by the intratumoral injection of a slow-release polymeric paste formulation of paclitaxel. Cancer Res 2000;60:4146–51.
43. Auzenne E, Donato NJ, Li C, et al. Superior therapeutic profile of poly-L-glutamic acid-paclitaxel copolymer compared with taxol in xenogeneic compartmental models of human ovarian carcinoma. Clin Cancer Res 2002;8:573–81.
44. Pucciarelli S, Codello L, Rosato A, Del Bianco P, Vecchiato G, Lise M. Effect of antiadhesive agents on peritoneal carcinomatosis in an experimental model. Br J Surg 2003;90:66–71.
45. Sandri G, Rossi S, Ferrari F, Bonferoni MC, Zerrouk N, Caramella C. Mucoadhesive and penetration enhancement properties of three grades of hyaluronic acid using porcine buccal and vaginal tissue, Caco-2 cell lines, and rat jejunum. J Pharm Pharmacol 2004;56:1083–90.